PHYSICAL REVIEW B VOLUME 23, NUMBER 4 15 FEBRUARY 1981

Self-consistent non-muffin-tin augmented-plane-wave calculation of the band structure of silicon

Frank Szmulowicz
University of Dayton Research Institute, Dayton, Ohio 45469
(Received 27 August 1980)

The augmented-plane-wave formalism of Rudge has been applied to the calculation of the band structure of silicon. Non-muffin-tin terms in the potential both inside and outside the muffin-tin radius have been included. The calculation has been carried out to self-consistency yielding a valence band in very good agreement with experiments. As in other first-principles calculations, the conduction band is only in qualitative agreement with experiment, although a better agreement is found for the non-self-consistent bands.

I. INTRODUCTION

The band structure of silicon has been calculated several times, although first-principles approaches have often been at variance with available experimental data.[1,2] The wide range of disagreement can be traced directly to the insufficient knowledge of the exchange-correlation potentials to be used in the one-electron band calculations.[3-5] The best calculations for silicon, in terms of agreement with the data, have been performed using empirical pseudopotentials.[6] These, of course, incorporate experimentally obtained information and utilize potentials in parametric form designed to reproduce observed interband transitions. Also, the price to be paid in these calculations is the loss of knowledge about the charge density giving rise to the potential.

The augmented-plane-wave (APW) method, in its standard muffin-tin (MT) form, is inappropriate in dealing with directionally bonded materials like silicon. Yet, the APW method possesses great attractiveness because its basic set of APW's in the MT region is energy dependent and thus has a large degree of variational freedom. Also, as in other first-principles approaches, it is always clear which charge density gives rise to the crystal potential.

In order to apply the APW method to semiconductors, non-MT corrections to the potential need to be included. DeCicco[7] suggested that the non-MT terms be decomposed into two parts: deviation from constant potential in the interstitial region, the so-called warped MT potential (WMT),[8] and nonspherical terms in the MT region. A few calculations with warped MT potentials using the APW method have been performed[7-13] as well as a few full non-MT potential APW calculations.[14-20]

The first APW calculation for a semiconductor by Keown for diamond used the standard MT formalism.[21] In order to obtain agreement with experiment for the band gap, Keown had to adjust the position of the MT zero of energy. This procedure must have been partly necessitated by the MT approximation. Recently Papaconstantopoulos and Klein used the MT formalism for silicon.[22] Their conclusion was that this approach does not yield any band gap for Si even if the calculation is carried to self-consistency. Only when the calculation was semiempirically adjusted, by shifting the $l=0$ logarithmic derivative of the radial wave function at the MT sphere radius, did the band gap appear.

A full non-MT calculation for silicon was performed with the self-consistent LAPW (linear APW) method by Hamann.[1] This method differs from the standard APW method in that it uses energy-independent APW's, thus eliminating the implicit energy dependence in APW secular determinants.[23] In a full non-MT APW calculation for Si, Kane[3,15] adopted an approach very close to that developed by Rudge for treating the non-MT corrections.[14] Kane's approach differs from that of Rudge in that it divides the potential into point charge, valence, and ionic (or core) contributions. The Hamiltonian for the valence electrons includes a term for the interaction with Si^{4+} ion cores and another for interaction with other valence electrons. The core potential is determined empirically by a fit to two lowest atomic energy levels of Si^{3+}. Also the core potential is assumed to be Coulombic outside atomic spheres. The valence-valence interaction is assumed to be given by a rapidly converging Fourier series with adjustable Fourier coefficients. The ionic charge is also taken as adjustable. Bands were calculated at a few high-symmetry points in the Brillouin zone (BZ) and the calculation was non-self-consistent.

In this paper, I apply Rudge's APW formalism,[14] with slight modifications to improve accuracy, to the calculation of the band structure of silicon. The calculation is fully non-MT, first-principles, and self-consistent. The potential is obtained from superposed atomic Si charge densities. The Coulomb part of the potential is obtained from the solution of the Poisson equation with the contribu-

tion of all multipole moments with $L \leq 7$ included. The exchange-correlation potential is of the $X\alpha$ form with $\alpha = 0.79$. The spherical harmonic expansion of the wave function in the MT region is carried out up to $l_{max} = 10$. The plane-wave-region (PW) expansion of the wave function in reciprocal-lattice wave vectors $\vec{K}_i$ is taken up to $|\vec{k}+\vec{K}_i| \leq (2\pi/a)4.5$, where a is the lattice constant. Potential in the PW region is Fourier expanded using first 112 $\vec{K}$-vector shells.

The present work aims to establish Rudge's non-MT APW formalism as a viable computational technique for semiconductors on the example of the band structure of Si. Its initial step involves calculations of certain Ewald sums which are no more complicated than the KKR (Korringa-Kohn-Rostoker) structure constants.[24,25] In fact, just like the KKR structure constants, these Ewald sums are common to all materials with the same lattice structure.

In Sec. II computational methods used in this self-consistent non-MT calculation are presented. Section III contains results and discussion of the band structure of Si. A summary is given in Sec. IV.

II. COMPUTATIONAL METHODS

A. Group-theoretical techniques

In constructing APW secular determinants, group theory can be used to considerably shorten the computational effort and increase its accuracy.[26,27] This section is devoted to presenting relevant notation used in subsequent developments.

The space group G for the diamond lattice is the nonsymmorphic space group O_h^7. The space group consists of operations of the form $\{R|\vec{t}_n+\vec{v}_R\}$, where R is a proper or improper rotation, $\vec{t}_n$ is a lattice translation, and $\vec{v}_R$ is a (minimal) nonprimitive fractional translation associated with R.[28] The group $G(\vec{k})$ of wave vector $\vec{k}$ consists of operations $\{R|\vec{t}_n+\vec{v}_R\}$ such that, in Slater's convention,[29]

$$\tilde{R}\vec{k} = \vec{k}+\vec{K}_m, \tag{1}$$

where $\tilde{R}$ is the transpose of R, and $\vec{K}_m$ is a reciprocal-lattice vector. Also, $G_0(\vec{k})$ will be used to denote the point group of the wave vector consisting of rotational parts of $G(\vec{k})$, and $\{G_0(\vec{k})\}$ denotes the reduced set of $G(\vec{k})$ consisting of $\{R|\vec{v}_R+\vec{t}_n\}$ with $\vec{t}_n = 0$.[30]

Koster has shown that the irreducible representation of the space group of the wave vector $G(\vec{k})$ for points interior to the BZ boundaries can be obtained from those of the $G_0(\vec{k})$ by the association

$$\Gamma^\alpha(\{R|\vec{t}_n+\vec{v}_R\}) = e^{i\vec{k}\cdot(\vec{t}_n+\vec{v}_R)}\Gamma^\alpha(R), \tag{2}$$

where on the left-hand side (LHS) we have the αth irreducible representation of $G(\vec{k})$ and on the right-hand side (RHS) that of the point group $G_0(\vec{k})$.[28] The main application of the full irreducible representations in this work is to provide projection operators for APW basis functions.[26,27,31] These functions satisfy the Bloch theorem, which simplifies the application of the projection operators. When operating on such functions the projection operator assumes the form

$$\rho_{ij}^\alpha = \sum_{\{G_0(\vec{k})\}} \Gamma_{ij}^\alpha(R)^* e^{-i\vec{k}\cdot\vec{v}_R}\{R|\vec{v}_R\}, \tag{3}$$

where the sum proceeds over g elements of the reduced set $\{G_0(\vec{k})\}$.[29,30]

For purposes of studying APW function's transformational properties they can be treated like plane waves as follows[27]:

$$\phi(\vec{k}_l,\vec{r}) = \exp[i(\vec{k}+\vec{K}_l)\cdot\vec{r}]. \tag{4}$$

The effect of the projection operator on these functions was considered by Slater.[29] In diamond, for points not on the UWX face of the BZ, he has shown that

$$\rho_{ij}^\alpha\phi(\vec{k}_l,\vec{r}) \equiv \phi_{ij}^\alpha(\vec{k}_l,\vec{r}) = \sum_{\{G_0(\vec{k})\}} \Gamma_{ij}^\alpha(R)^* e^{i\vec{R}\vec{k}_l\cdot\vec{v}_R} e^{i\vec{R}\vec{k}_l\cdot\vec{r}}. \tag{5}$$

A computer program was set up to perform the operations in Eq. (5) using the tables of irreducible representations given by Slater.[32] The output consists of linearly independent symmetrized basis functions for all symmetry points other than those on the UWX face of the BZ. As shown by Mattheiss *et al.*, this requires the application of only the ρ_{11}^α projection operator.[27] With this list of symmetrized APW's the secular determinant could be simplified with the use of the following orthogonality relation[26,27]:

$$\langle\phi_{11}^\alpha(\vec{k}_l,\vec{r})|(H-E)|\phi_{11}^\alpha(\vec{k}_m,\vec{r})\rangle \equiv (H-E)_{lm}^\alpha = (g/n_\alpha)\langle\phi(\vec{k}_l,\vec{r})|(H-E)|\phi_{11}^\alpha(\vec{k}_m,\vec{r})\rangle, \tag{6}$$

where n_α is the dimensionality of the irreducible representation Γ^α of $G_0(\vec{k})$, and E the energy.

In dealing with points on the UWX face of the BZ the present program uses points of lower symmetry located very close to those on the UWX face. For point X the program calculates bands and wave functions on the Δ axis at $(2\pi/a)(0.999, 0, 0)$, for W, on the Q axis at $(2\pi/a)(0.999, 0.5, 0.001)$, and for the midpoint of the Z axis it uses the point on the ΓKWX plane at $(2\pi/a)(0.999, 0.25, 0.0)$. Often, but not always, compatibility relations can be used to determine the irreducible

representation of the corresponding band on the Z axis. All eigenvalues at X, Z, and W are doubly degenerate so it usually takes two bands off the axis to "make up" one band on the axis. The two bands are of different symmetries and are calculated independently. Invariably, they were within 0.001 Ry of one another, which serves as an indication of the calculation's convergence.

B. The non-muffin-tin APW method

In the APW method, originally proposed by Slater[33] in 1937, the wave function in the PW region is expanded in plane waves as follows:

$$\phi(\vec{k}_i,\vec{r})=\exp(i\vec{k}_i\cdot\vec{r}),\quad |\vec{r}-\vec{r}_\nu|>R_M \tag{7}$$

where $\vec{k}_i=\vec{k}+\vec{K}_i$, $\vec{k}$ is a wave vector in the BZ, R_M the MT sphere radius, and $\vec{K}_i$ a reciprocal-lattice wave vector. In the MT region the Bloch wave function is expanded in terms of solutions to the radial Schrödinger equation $u_l(|\vec{r}-\vec{r}_\nu|)$, where $\vec{r}_\nu=\pm\frac{1}{8}a(1,1,1)$ labels the position of a νth atom in the unit cell, as

$$\phi(\vec{k}_i,\vec{r})=4\pi\exp(i\vec{k}_i\cdot\vec{r}_\nu)\sum_{l,m} i^l j_l(k_iR_M)Y_{lm}(\vec{k}_i)^*Y_{lm}(\vec{r}-\vec{r}_\nu)u_l(|\vec{r}-\vec{r}_\nu|)/u_l(R_M),\quad |\vec{r}-\vec{r}_\nu|\le R_M. \tag{8}$$

Here j_l is a spherical Bessel function and Y_{lm} a spherical harmonic.[34] The total Bloch wave function is given by the expansion of these augmented-plane waves,

$$\psi(\vec{k},\vec{r})=N^{-1/2}\sum_i v_i\phi(\vec{k}_i,\vec{r}), \tag{9}$$

where v_i are variational coefficients and N is a normalization constant.[27]

The present calculation patterns itself after the formalism developed by Rudge for the non-muffin-tin APW method.[14] The potential is expanded in cubic harmonics in the MT region as

$$V(\vec{r})=\sum_{L\nu} V_L(|\vec{r}-\vec{r}_\nu|)W_{L\nu}(\vec{r}-\vec{r}_\nu),\quad |\vec{r}-\vec{r}_\nu|\le R_M \tag{10}$$

where $W_{L\nu}$ is the Lth cubic harmonic transforming like the Γ_1 representation of the T_d group for the νth atom in the diamond unit cell. In the interstitial region

$$V(\vec{r})=\sum_{\vec{K}} V(\vec{K})e^{i\vec{K}\cdot\vec{r}}=\sum_{\vec{K}} V_s(\vec{K})e^{i\vec{K}\cdot\vec{r}}, \tag{11}$$

where the first reciprocal-lattice series is not unique. The $V_s(\vec{K})$ series is unique since it is chosen so that it is identically zero inside each MT sphere. In the present calculation the first series, which is rapidly converging, was summed over 112 $\vec{K}$-vector shells. The second, slowly converging series, was summed over the first 55 shells of $\vec{K}$ vectors. The muffin-tin radius was chosen to be half the nearest-neighbor distance. Standard midpoint origin is used in order to obtain real secular determinants.

C. Secular determinant

Specializing Rudge's expressions to the case of the diamond lattice the secular equation can be written as follows[27]:

$$\Omega^{-1}(H-E)^\alpha_{ij}=-EA^\alpha_{ij}+B^\alpha_{ij}+\sum_{l=0}^{l_{\max}} C^\alpha_{ijl}[u_l'(R_M)/u_l(R_M)]+\sum_{l,l'=0}^{l_{\max}}\sum_L D^\alpha_{ij,ll'L}\left(\int_0^{R_M}[u_{l'}(r)/u_{l'}(R_M)]V_L(r)[u_l(r)/u_l(R_M)]r^2dr\right). \tag{12}$$

In Eq. (12) Ω is the unit-cell volume,

$$A^\alpha_{ij}=\frac{g}{n_\alpha}\sum_{\{R|\vec{v}_R\}}\Gamma^\alpha_{11}(R)^*e^{i\vec{R}_j\cdot\vec{v}_R}\left\{\delta(\vec{k}_i,\vec{R}\vec{k}_j)-(4\pi R_M^2/\Omega_0)\cos[(\vec{R}\vec{k}_j-\vec{k}_i)\cdot\tfrac{1}{2}\vec{d}]\frac{j_1(|\vec{R}\vec{k}_j-\vec{k}_i|R_M)}{|\vec{R}\vec{k}_j-\vec{k}_i|}\right\}, \tag{13}$$

$$B^\alpha_{ij}=\frac{g}{n_\alpha}\sum_{\{R|\vec{v}_R\}}\Gamma^\alpha_{11}(R)^*e^{i\vec{R}_j\cdot\vec{v}_R}[(\vec{k}_i\cdot\vec{R}\vec{k}_j)\{\cdots\}+V_s(\vec{k}_i-\vec{R}\vec{k}_j)], \tag{14}$$

where the curly bracket is the same as in Eq. (13), $\Omega_0=\frac{1}{2}\Omega$, $\vec{d}=\frac{1}{4}a(1,1,1)$, and

$$C^\alpha_{ijl}=(g/n_\alpha)(4\pi R_M^2/\Omega_0)(2l+1)j_l(k_iR_M)j_l(k_jR_M)\times\sum_{\{R|\vec{v}_R\}}\Gamma^\alpha_{11}(R)^*e^{i\vec{R}_j\cdot\vec{v}_R}\cos[(\vec{R}\vec{k}_j-\vec{k}_i)\cdot\tfrac{1}{2}\vec{d}]P_l(\vec{R}\vec{k}_j\cdot\vec{k}_i), \tag{15}$$

with P_l being the Legendre polynomial. Exclusion of the last term in Eq. (12) results in the warped muffin-tin formalism.[8]

The last term is the most complicated. It is given by

$$D^{\alpha}_{ij,\,ll'L}=\frac{g}{n_\alpha}\frac{4\pi}{\Omega_0}\sum_{\{R|\vec{v}_R\}}\Gamma^{\alpha}_{11}(R)^* e^{i\vec{R}_j\cdot\vec{v}_R} \times j'_l(k_iR_M)j_{l'}(k_jR_M)F_{ll'L}(\vec{k}_i,\vec{R}\vec{k}_j)\times\begin{cases}\cos[(\vec{R}\vec{k}_j-\vec{k}_i)\cdot\vec{r}], & L \text{ even}\\ \sin[(\vec{R}\vec{k}_j-\vec{k}_i)\cdot\vec{r}], & L \text{ odd},\end{cases} \tag{16}$$

where

$$F_{ll'L}=4\pi i^{l-l'}\sum_{m,m'}Y_{l'm'}(\vec{k}_i)Y^*_{lm}(\vec{R}\vec{k}_j)\int d\Omega\, Y^*_{l'm'}(\vec{r})W_L(\vec{r})Y_{lm}(\vec{r})\times\begin{cases}1, & L \text{ even}\\ -i, & L \text{ odd}.\end{cases} \tag{17}$$

involves angular functions only. This term arises from the first-order perturbative treatment of the nonspherical contribution to the potential in the MT region.

In evaluating the energy-independent coefficients, symmetry considerations were employed to obtain a number of useful relations. The Fourier coefficients of the potential are related by

$$V(R\vec{K})=(\cos R\vec{K}\cdot\vec{v}_R)V(\vec{K}) \tag{18}$$

for $\{R|\vec{v}_R\}$ in the reduced set of the space group. For R in point group T_d it can be shown that

$$V(R\vec{K})=[\cos(\vec{K}-R\vec{K})\cdot\tfrac{1}{2}\vec{d}]V(\vec{K}), \tag{19}$$

and for R in IT_d, where I is the inversion operator,

$$V(R\vec{K})=[\cos(\vec{K}+R\vec{K})\cdot\tfrac{1}{2}\vec{d}]V(\vec{K}). \tag{20}$$

The triple sum over l, l', and L was evaluated for $L=0$, 3, 4, 6, 7 and $l,l'\leq 4$, resulting in 15 integrals. All angular integrals in $F_{ll'L}(\vec{k}_i,\vec{R}\vec{k}_i)$ have been worked out with the aid of Clebsch-Gordan coefficients. Results were cast into forms containing cubic harmonics as these, being in Cartesian form, are easily generated. The relevant results are summarized in Table I.

The energy-independent coefficients A^{α}_{ij}, B^{α}_{ij}, $C^{\alpha}_{ij\,l}$, and $D^{\alpha}_{ij,\,ll'L}$ were stored on tape for quick retrieval, thereby obviating the need for generating them each time the secular determinant is evaluated.[27] The energy-dependent quantities $u'_l(R_M,E)/u_l(R_M,E)\equiv L_l(E)$, otherwise known as the logarithmic derivatives of the radial wave functions, up to $l_{\max}=10$ were fitted to a 10th-degree polynomial in E.[24] Similarly, the required 15 integrals multiplying $D^{\alpha}_{ij,\,ll'L}$ were fitted to the same-order polynomial.

D. Construction of the starting potential

The starting potential was constructed by the method originally suggested by Mattheiss for MT potentials.[35] The atomic charge density for Si in the $3s^13p^3$ configuration was evaluated on a 250-point logarithmic mesh using the Hartree-Fock–Slater self-consistent field program of Desclaux.[36] This mesh expands the scale near the nucleus, where most rapid variations of the radial wave functions occur. The spherical charge density from the program, $\rho_{\rm at}(r)$, was then placed at each atomic site and superposed to yield the crystal charge density

$$\rho_{\rm crystal}(\vec{r})=\sum_{\vec{R}}[\rho_{\rm at}(\vec{r}-\vec{R}-\vec{r}_1)+\rho_{\rm at}(\vec{r}-\vec{R}-\vec{r}_2)], \tag{21}$$

where $\vec{R}$ are direct fcc lattice vectors and $\vec{r}_{1,2}=\pm(\frac{1}{8}a)(1,1,1)$ are positions of Si atoms in the unit cell. The lattice constant was taken to be $a=5.431$ Å, $R_M=2.222$ a.u.

In the PW region the crystal charge density was Fourier decomposed:

$$\rho_{\rm crystal}(\vec{r})=\sum_{\vec{K}}\rho(\vec{K})\exp(i\vec{K}\cdot\vec{r}), \tag{22}$$

where

$$\rho(\vec{K})=[4\pi\cos\tfrac{1}{2}(\vec{K}\cdot\vec{d})/\Omega_0]\int_0^{\infty}dr\,r^2j_0(Kr)\rho_{\rm at}(r). \tag{23}$$

Since the plane-wave expansion in the PW region is not unique it was convenient to evaluate the radial integral with $\rho_{\rm at}(r)$ fitted to a form Ar^2+Br^3 for $r\leq R_M$ to speed the convergence of the series.[19] For $r\geq R_M$ the actual form of $\rho_{\rm at}(r)$ was used, which is joined continuously by the Ar^2+Br^3 form inside R_M. In actual construction of the potential, 210 shells of $\vec{K}$ vectors were used to construct 112 $V(\vec{K})$ coefficients and 55 $V_s(\vec{K})$ Fourier components.

In the MT region the crystal charge density was expanded in cubic harmonics of Von der Lage and Bethe as[37]

$$\rho_{\rm crystal}(\vec{r})=\sum_{L\nu}\rho_L(|\vec{r}-\vec{r}_\nu|)W_{L\nu}(\vec{r}-\vec{r}_\nu). \tag{24}$$

The $\rho_L(r)$ coefficients were evaluated using the Löwdin alpha expansion[38]

TABLE I. Reduction of Eq. (17) to sums over cubic harmonics of Von der Lage and Bethe (Ref. 37). Einstein sum over index $m = x, y, z$, or $m = 1, 2$ for the γ harmonics, is implicitly assumed.

L	l	l'	$F_{ll'L}(\vec{k}_i, \vec{R}\vec{k}_i)$
3	0	3	$\beta_3(\vec{k}_i)\alpha_0(\vec{R}\vec{k}_j)$
3	1	2	$-\sqrt{3/7}\,\epsilon_{2m}(\vec{k}_i)\delta_{1m}(\vec{R}\vec{k}_j)$
3	1	4	$2/\sqrt{7}\,\epsilon_{4m}(\vec{k}_i)\delta_{1m}(\vec{R}\vec{k}_j)$
3	2	3	$2/3\delta_{3m}(\vec{k}_i)\epsilon_{2m}(\vec{R}\vec{k}_j)$
3	3	4	$2\sqrt{21}/11\alpha_4(\vec{k}_i)\beta_3(\vec{R}\vec{k}_j)$
			$+\sqrt{3}/11\epsilon_{4m}(\vec{k}_i)\delta_{3m}(\vec{R}\vec{k}_j) - \sqrt{35}/11\delta'_{4m}(\vec{k}_i)\epsilon'_{3m}(\vec{R}\vec{k}_j)$
4	0	4	$\alpha_4(\vec{k}_i)\alpha_0(\vec{R}\vec{k}_j)$
4	1	3	$-2/3\delta_{3m}(\vec{k}_i)\delta_{1m}(\vec{R}\vec{k}_j)$
4	2	2	$-2/\sqrt{21}\epsilon_{2m}(\vec{k}_i)\epsilon_{2m}(\vec{R}\vec{k}_j) + \sqrt{3/7}\,\gamma_2^m(\vec{k}_i)\gamma_2^m(\vec{R}\vec{k}_j)$
4	2	4	$10/(11\sqrt{7})[\epsilon_{4m}(\vec{k}_i)\epsilon_{2m}(\vec{R}\vec{k}_j) - 2\gamma_4^m(\vec{k}_i)\gamma_2^m(\vec{R}\vec{k}_j)]$
4	3	3	$\sqrt{7}/(11\sqrt{3})[-6\beta_3(\vec{k}_i)\beta_3(\vec{R}\vec{k}_j) + 3\delta_{3m}(\vec{k}_i)\delta_{3m}(\vec{R}\vec{k}_j)$
			$-\epsilon'_{3m}(\vec{k}_i)\epsilon'_{3m}(\vec{R}\vec{k}_j)]$
4	4	4	$27\sqrt{7}/(11\sqrt{3})[2/13\alpha_4(\vec{k}_i)\alpha_4(\vec{R}\vec{k}_j) - 1/7\epsilon_{4m}(\vec{k}_i)\epsilon_{4m}(\vec{R}\vec{k}_j)$
			$+1/13\delta'_{4m}(\vec{k}_i)\delta'_{4m}(\vec{R}\vec{k}_j) + 2/91\gamma_4^m(\vec{k}_i)\gamma_4^m(\vec{R}\vec{k}_j)]$
6	2	4	$-5\sqrt{6}/(22\sqrt{13})[4\epsilon_{4m}(\vec{k}_i)\epsilon_{2m}(\vec{R}\vec{k}_j) + 3\gamma_4^m(\vec{k}_i)\gamma_2^m(\vec{R}\vec{k}_j)]$
6	3	3	$10/(11\sqrt{26})[4\beta_3(\vec{k}_i)\beta_3(\vec{R}\vec{k}_j) + 5/3\delta_{3m}(\vec{k}_i)\delta_{3m}(\vec{R}\vec{k}_j)$
			$-3\epsilon'_{3m}(\vec{k}_i)\epsilon'_{3m}(\vec{R}\vec{k}_j)]$
6	4	4	$\sqrt{2}/(11\sqrt{13})[20\alpha_4(\vec{k}_i)\alpha_4(\vec{R}\vec{k}_j) - 16\gamma_4^m(\vec{k}_i)\gamma_4^m(\vec{R}\vec{k}_j)$
			$+5\epsilon_{4m}(\vec{k}_i)\epsilon_{4m}(\vec{R}\vec{k}_j) - \delta'_{4m}(\vec{k}_i)\delta'_{4m}(\vec{R}\vec{k}_j)]$
7	3	4	$1/(11\sqrt{39})[-3\sqrt{105}\,\delta'_{4m}(\vec{k}_i)\epsilon'_{3m}(\vec{R}\vec{k}_j) - 35\epsilon_{4m}(\vec{k}_i)\delta_{3m}(\vec{R}\vec{k}_j)$
			$-15\sqrt{7}\,\alpha_4(\vec{k}_i)\beta_3(\vec{R}\vec{k}_j)]$

$$\rho_L(r) = \rho_{\rm at}(r)\delta_{Lo} + \left\{\sum_{\vec{R}\neq 0,\ \vec{d}=0} + \sum_{\vec{R}}\right\} W_L(\vec{R}+\vec{d})\frac{1}{2|\vec{R}+\vec{d}|\,r}\int_{||\vec{R}+\vec{d}|-r|}^{|\vec{R}+\vec{d}|+r} dr' r' \rho_{\rm at}(r') P_L\left(\frac{|\vec{R}+\vec{d}|^2 + r^2 - r'^2}{2|\vec{R}+\vec{d}|\,r}\right). \tag{25}$$

The first sum proceeds over atoms lattice translation away from the central atom at $r = 0$. The second sum proceeds over the other atoms in the basis. Altogether, the sum was performed over 71 shells of atoms. All radial integrals in (23) and (25) were computed with a 96-point Gaussian quadrature. As a check, the two series were resummed at the midpoint origin. The continuity of charge across the MT boundary was satisfied to within 0.1%.

With the charge density obtained above, the Coulomb part of the potential was obtained using Rudge's formulas from Sec. V of his paper.[14] The potential consists of three parts, each of which was calculated and checked separately for continuity. The last part of this potential is due to an ordered array of point multipoles. The coefficients for the resulting generalized Ewald potential problems were calculated in the preceding paper.[39]

The exchange-correlation potential was taken to be of the $X\alpha$ form

$$V_{\rm xc}(\vec{r}) = -3\alpha(3/\pi)^{1/3}[\rho(\vec{r})]^{1/3}, \tag{26}$$

where from previous work on silicon by M. L. Cohen and co-workers[40] α was chosen to be 0.79. This value for α brings the $V_{\rm xc}$ into agreement with Wigner's interpolation formula at the average valence charge density of silicon.[41]

Since $\rho_0(r)$ is the dominant radial component of the MT charge density, $V_{\rm xc}(\vec{r})$ can be expanded to good accuracy in binomial series yielding cubic harmonic decomposition of $V_{\rm xc}$ for $r \leq R_M$.[14] No such expansion is possible for $r > R_M$. Here I use

a three-dimensional finite Fourier transform[42]

$$V_{xc}(\vec{K}) = (2N+1)^{-3} \sum_{n,l,m} V_{xc}(\vec{r}_{nlm}) \exp(-i\vec{K}\cdot\vec{r}_{nlm}), \quad (27)$$

where

$$\vec{r}_{nlm} = (n\vec{R}_1 + l\vec{R}_2 + m\vec{R}_3)/(2N+1) \quad (28)$$

and $\vec{R}$'s are primitive fcc translation vectors. We now have

$$\vec{K} = i\vec{K}_1 + j\vec{K}_2 + k\vec{K}_2, \quad (29)$$

with

$$-N \leq n, l, m, i, j, k \leq N, \quad (30)$$

and $N = 11$. The sum was carried out over $\frac{1}{24}$th of the unit cell, taking advantage of the T_d point-group symmetry about any atom in the cell, using about 720 $\vec{r}_{nlm}$. The $V_{xc}(\vec{r})$ was calculated using $\rho(\vec{r})$ in the Fourier-series form, Eq. (22), which was then continued into the MT spheres when necessary. This procedure is legitimate since the Fourier coefficients $V(\vec{K})$ in Eq. (11) are not unique.

E. Approaching self-consistency

After the first iteration with the potential constructed from the superposed charge density the new charge densities were obtained from the band-wave functions. The valence bands and wave functions were calculated at six equally spaced points in the BZ—Γ, X, L, W, halfway along the Δ axis, and along the Σ axis at $(2\pi/a)(\frac{1}{2}, \frac{1}{2}, 0)$.[2,42] Wave functions were expanded in APW's with $|\vec{k}+\vec{K}_t| \leq (2\pi/a)4.5$ to obtain good convergence for the conductions bands. This corresponds to 113 plane waves at Γ. Inside the MT spheres the spherical harmonic expansion of the wave function was carried out to $l_{max} = 10$. Matrix elements of the non-muffin-tin corrections to the potential were performed using $V_s(\vec{K})$ from the first 55 $\vec{K}$ shells and for $V_L(r)$ with $L = 0, 3, 4, 6, 7$ and $l, l' \leq 4$. While constructing these potentials, $\vec{K}$ sums were done with the first 112 $\vec{K}$-vector shells. It was found that these many terms were sufficient for convergence of $V(\vec{K})$, $\rho(\vec{K})$, Q_l (multipole moments of the charge distribution), and for other quantities derivable from $\vec{K}$ sums.

Secular determinants were solved by Gaussian elimination with complete pivoting.[43] The variational coefficients v_i were obtained then by back substitution. The wave functions were properly normalized using the identity[27,34]

$$N_{\vec{k}\alpha} = \Omega \sum_{i,j} v_i v_j \left(A^{\alpha}_{ij} - \sum_l C^{\alpha}_{ijl} \frac{d}{dE} L_l(E) \right), \quad (31)$$

where all the quantities have been previously stored. From now on v_i will be taken as normalized.

From each valence-band wave function, the part transforming like the Γ_1 representation of the space group at the center of the BZ was projected out. With the aid of the projection operator ρ^{Γ_1}, the Γ_1 part of the charge density is given by

$$\rho^{\Gamma_1} |\psi^{\alpha}(\vec{k}, r)|^2 \equiv \sum_{\vec{K}} \rho^{\alpha}_{\vec{k}}(\vec{K}) e^{i\vec{K}\cdot\vec{r}} \quad (32)$$

in the interstitial region. For $\vec{k}$ not on the UWX face of the BZ

$$\rho^{\alpha}_{\vec{k}}(\vec{K}) = \frac{g}{Gn_{\alpha}} \sum_{i,j} v_i v_j \sum_{\{T|\vec{v}_t\}} \Gamma^{\alpha}_{11}(T)^* e^{i\vec{K}_j\cdot\vec{v}_t} \left(\sum_{\{S|\vec{v}_s\}} e^{i(\vec{T}\vec{k}_j - \vec{k}_i)\cdot\vec{v}_s} \delta(\vec{T}\vec{k}_j - \vec{k}_i, S\vec{K}) \right), \quad (33)$$

where $\{T|\vec{v}_t\} \in \{G_0(\vec{k})\}$ and $G = 48$ operations $\{S|\vec{v}_s\}$ are in $\{G_0(\vec{k}=0)\}$.

In the MT region the charge distribution $|\psi^{\alpha}(\vec{k}, \vec{r})|^2$ was decomposed into its Γ_1 cubic harmonic contributions. This is accomplished by the angular integration

$$\rho^{\alpha}_L(\vec{k}, \vec{r}) = (4\pi)^{-1} \int W_L(\vec{r}) |\psi^{\alpha}(\vec{k}, \vec{r})|^2 d\Omega. \quad (34)$$

For $L = 0$

$$\rho^{\alpha}_0(\vec{k}, \vec{r}) = \frac{\Omega_0}{4\pi R_M^2} \sum_{i,j} v_i v_j \sum_l C^{\alpha}_{ijl} \left(\frac{u_l(r)}{u_l(R_M)} \right)^2, \quad (35)$$

while for $L \neq 0$

$$\rho^{\alpha}_L(\vec{k}, r) = \frac{\Omega_0}{4\pi} \sum_{i,j} v_i v_j \sum_{l,l'} D^{\alpha}_{ij,ll'L} \frac{u_l(r) u_{l'}(r)}{u_l(R_M) u_{l'}(R_M)}, \quad (36)$$

where again C and D have been previously stored.

The total $\rho(\vec{r})$ was obtained from the six $\vec{k}$-point sum

$$\rho(\vec{K}) = 2 \sum_{\vec{k}} \sum_{\alpha} n_{\alpha} \rho^{\alpha}_{\vec{k}}(\vec{K}) W_{\vec{k}}, \quad r > R_M \quad (37)$$

and

$$\rho_L(r) = 2 \sum_{\vec{k}} \sum_{\alpha} n_{\alpha} \rho^{\alpha}_L(\vec{k}, \vec{r}) W_{\vec{k}}, \quad r \leq R_M \quad (38)$$

where $W_{\vec{k}}$ are weight factors accounting for the irreducible wedge volume nearest to the given $\vec{k}$. The six points used here were also employed by Euwema *et al.*,[42] who found them to be representative of the whole zone.

The potential was then constructed from $\rho(\vec{r})$ above just as that described in Section IID for

the non-self-consistent potential. At the same time as the valence bands were iterated toward self-consistency the core levels were also recalculated. A simple scheme was used to calculate core radial wave functions for the $1s$, $2s$, and $2p$ levels. The radial Schrödinger equation was integrated toward R_M using the spherical part of the potential $V_0(r)$. The boundary condition setting the radial wave functions to zero at R_M determined the core energy levels.

III. RESULTS AND DISCUSSION

The APW band structure was iterated to self-consistency in four cycles, recomputing each time the valence as well as the core level charge density. The number of cycles is a function of the caution employed in approaching the self-consistency criterion which was 0.01 eV, or 0.001 Ry. This criterion corresponds to the estimated numerical accuracy of the calculation. In presenting results it will be of interest to compare outputs of both the self-consistent (SCAPW) and non-self-consistent (NSCAPW) band structures.

Figure 1 shows the starting atomic charge density and the $L=0$ components of both the superposed and self-consistent crystal charge density. The iteration process is seen to have the effect of charge rearrangement in the unit cell as charge "flows" to the outer regions of each muffin-tin sphere. Figures 2 and 3 emphasize the importance of nonspherical contributions to the charge density and the need for a self-consistent treatment in the calculation. As expected, ρ_3, ρ_4, ρ_6, and ρ_7 are present in this order of importance. Each of these components can be seen to penetrate into the MT spheres with higher L components penetrating less than the lower ones. The self-consistency process has enhanced the ρ_3 and ρ_4 components while decreasing the ρ_6 and ρ_7 densities

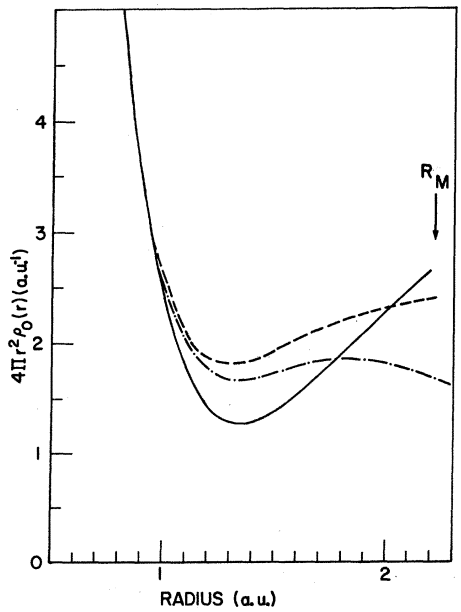

FIG. 1. Spherical component of silicon's charge density. The dash-dot lines give the free atomic density, the dashed lines the superposed charge crystal density, and the continuous curve the converged SCAPW charge density.

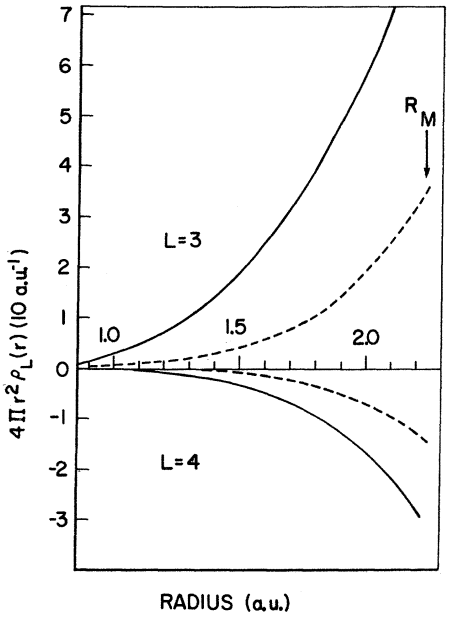

FIG. 2. $L=3$ and 4 nonspherical components for the superposed charge model (dashed lines) and the SCAPW crystal charge density (solid lines) of silicon.

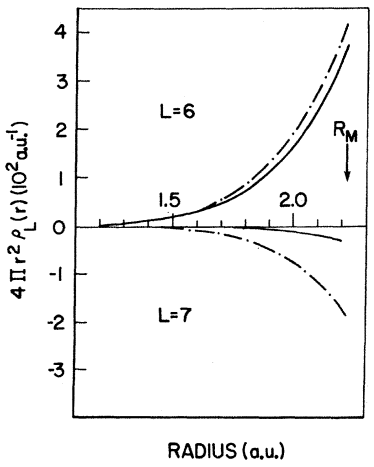

FIG. 3. $L=6$ and 7 nonspherical components of the superposed (dashed lines) and the SCAPW (solid lines) Si crystal charge density.

in comparison with the overlapped values. The rapid increase of the ρ_L for $L \neq 0$ near R_M suggests that extension of the cubic harmonic expansion outside the MT spheres would be inappropriate. This series would require a large number of high L components and thus be difficult to converge.

Figure 4 presents the total crystal charge density along the [111] bond direction and its decomposition into the valence and core contributions. The valence charge density near midbond in this plot is in good qualitative agreement with soft-core pseudopotential valence charge density calculated by Hamann.[1] The soft-core charge density is also in good accord with that calculated from local empirical pseudopotential by Walter and Cohen.[44] Conversely, the present results in Fig. 4 do not exhibit a large flat region near the midbond position as do the LAPW and hard-core valence charge densities calculated by Hamann. Near the core in Fig. 4 the valence charge density drops faster than the soft-core density. This is in greater accord with Hamann's hard-core valence charge density. The most significant difference in our two calculations is the use by Hamann of the Wigner interpolation formula for the exchange and correlation potential.[41] It will be seen later that this results in conduction bands quite different from those calculated here.

The Fourier components of the charge density in the PW region will not be given here as they do not provide much information. As is well known, the plane-wave basis set is overcomplete outside the MT spheres so that the Fourier coefficients are not uniquely defined in the absence of an extra constraint.

Figures 5 and 6 give the plots of both the spherical and nonspherical terms in the potential. The dominant term is the $L=0$ component until the MT radius is reached, where nonspherical components, especially $L=3$ and 4, become significant. The largest effect of the self-consistency requirement is to enhance V_3 and shorten its range. Additionally, $V_0(r)$ undergoes a rather uniform downward shift, making the potential more attractive. Table II presents the first twenty-four Fourier components of the potential in the PW region to demonstrate their manifest nonconvergence. These coefficients are unique since a constraint has been imposed on the series by requiring it to vanish in each MT region. The nonconvergence does not present any problems

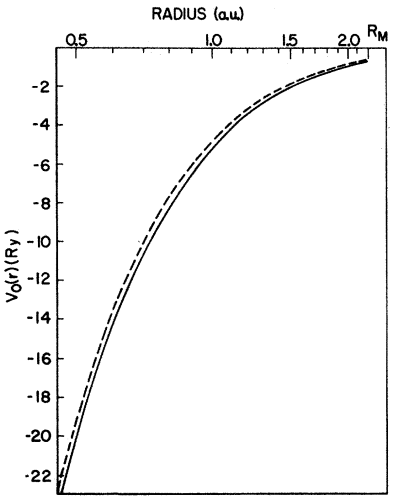

FIG. 5. Spherical component of the superposed model (dashed lines) and the SCAPW (solid line) Si crystal potential.

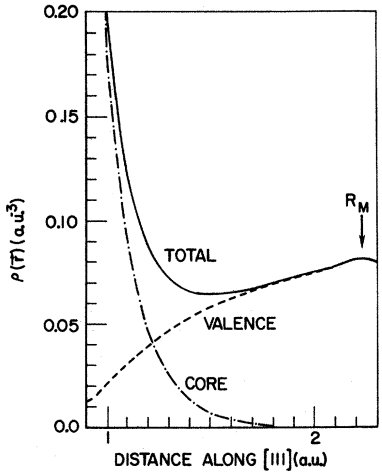

FIG. 4. Valence, core, and total crystal charge densities along the [111] bonding direction from the SCAPW calculation.

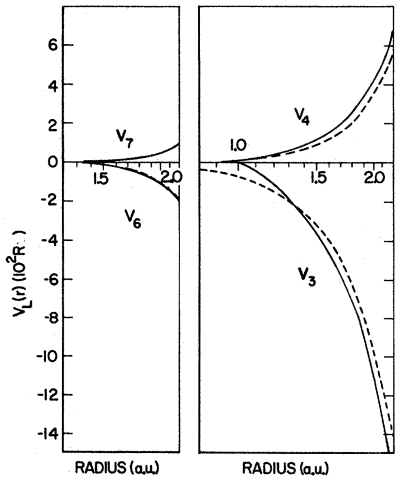

FIG. 6. Nonspherical components of the superposed charge model (dashed lines) and the SCAPW (full curve) Si crystal potential.

TABLE II. First twenty-five Fourier coefficients of the step potential in the interstitial region for the overlapped charge model and the self-consistent potential.

$(a/2\pi)\vec{K}$			$V_s(\vec{K})$ in Ry	
			Overlapped	SCAPW
0	0	0	0.0	0.0
1	1	1	0.043 11	0.052 33
2	0	0	0.0	0.0
2	2	0	−0.031 22	−0.038 73
3	1	1	−0.008 94	−0.010 23
2	2	2	0.012 78	0.015 71
4	0	0	0.006 25	0.008 11
3	3	1	−0.002 11	−0.003 06
4	2	0	0.0	0.0
4	2	2	−0.010 86	−0.013 03
5	1	1	−0.007 90	−0.009 23
3	3	3	−0.008 48	−0.010 16
4	4	0	−0.003 36	−0.003 72
5	3	1	−0.000 58	−0.000 54
4	4	2	0.000 31	0.000 35
6	0	0	0.0	0.0
6	2	0	0.002 50	0.003 16
5	3	3	−0.001 82	−0.002 32
6	2	2	0.001 32	0.001 51
4	4	4	−0.005 11	−0.006 29
5	5	1	−0.003 53	−0.004 08
7	1	1	0.004 58	0.005 37
6	4	0	0.0	0.0
6	4	2	−0.004 47	−0.005 22

in the calculation, since only low $\vec{K}$ components of $V_s(\vec{K})$ are ever needed. This is due to the fact that the APW's $\phi(\vec{k}_i, \vec{r})$ for high $\vec{K}_i$ do not make significant contributions for states in the valence band and low excited states in the conduction band.

Figures 7 and 8 display the non-self-consistent and self-consistent energy bands of silicon, respectively, calculated by the APW method. The qualitative aspects of the two band structures are quite similar. Even the transposition of the Γ_2' and Γ_{15} bands between the plots does not alter the band shapes along the symmetry axes.

The most striking difference between the two plots is the twofold increase in the band gap as the result of the self-consistent treatment. The effect can be attributed to changes of the exchange-correlation potential used here, which is proportional to $(-\alpha\rho^{1/3})$. From Figs. 1, 2, and 3 it can be seen that the charge density starts accumulating in the outer regions of the MT spheres and, from continuity, also in the PW region. Therefore, the exchange-correlation potential becomes more attractive for delocalized states like the bonding valence states. Conversely, for antibonding localized states in the conduction band the potential becomes less attractive or more repulsive. This accounts for the overall downward shift of the valence bands and upward shift of the conduction bands. The total effect pulls the valence and conduction bands apart, resulting in an abnormally large band gap.

Another argument can be made by examining Fig. 6 for V_3. As a result of self-consistency, V_3 grows larger and becomes shorter range. In the [111] bond direction, $V_3(r)$ becomes more attractive for bonding states in the valence band. In nonbonding directions $[\bar{1}11], [1\bar{1}1], [11\bar{1}], [\bar{1}\bar{1}\bar{1}]$ the contribution of $V_3(r)W_3(\vec{r})$ is positive because of of the sign of $W_3(\vec{r})$. Therefore, as a result of

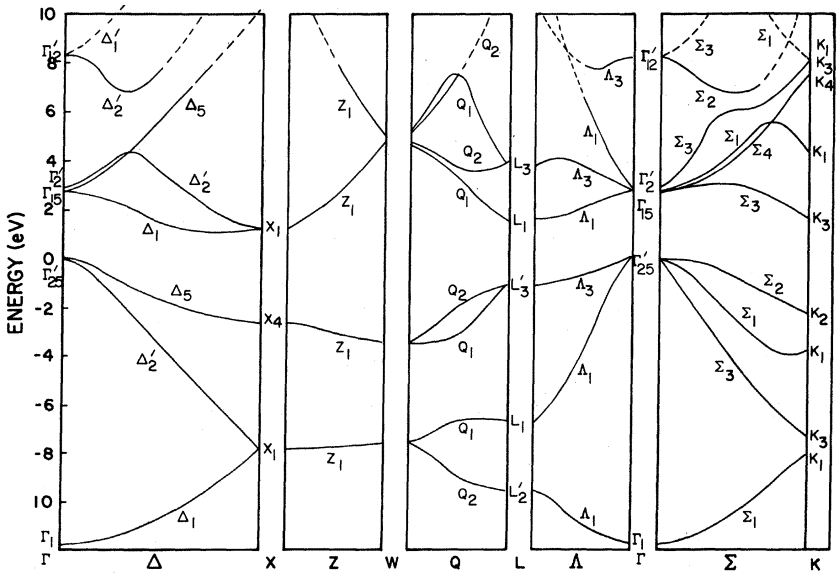

FIG. 7. Non-self-consistent energy-band structure of silicon using the superposed charge potential and the non-muffin-tin APW method.

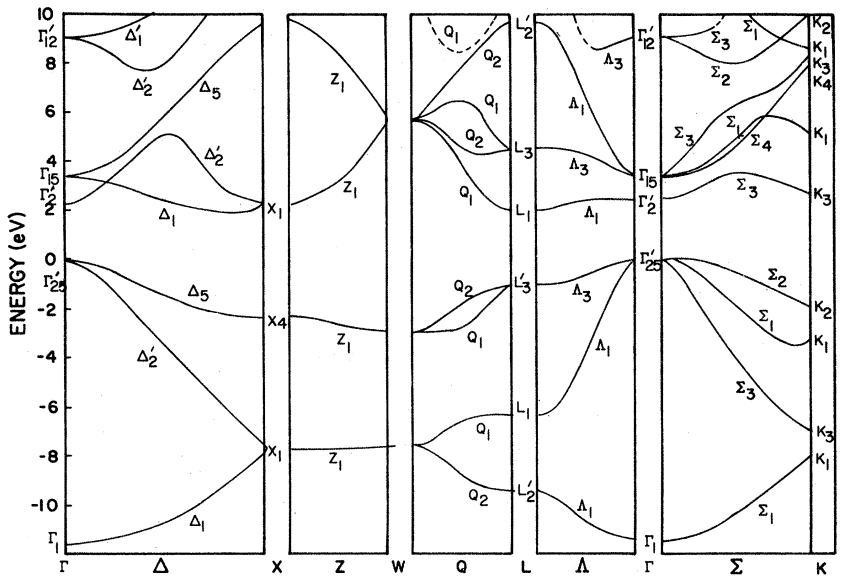

FIG. 8. Self-consistent energy-band structure of silicon using the non-muffin-tin APW method.

self-consistency, the total potential in nonbonding directions grows more repulsive. But these are also the regions where some of the conduction-band states have large amplitudes. One can conclude that the gap should increase as valence charge accumulates along the bonds. Finally, like Stukel *et al.*[45-47] I find that the self-consistency does have the effect of compressing the valence band.

A possible fix for the current problem could be a decrease in the exchange-correlation coefficient α to around 0.66.[45-47] This most certainly would improve the band gap and the positions of the Γ_2' and Γ_{15} levels. Given the present lack of knowledge of reliable excitation potentials this approach might be a partial solution to the problem.[1]

It is interesting to note that the NSCAPW results are in good agreement with experiment, and also with the empirical pseudopotential,[6] for the valence band. To a lesser degree the same can be said of the conduction bands except for Γ_{15} and Γ_2'. The NSCAPW bands give the correct band gap, which is a minimum requirement for any calculation. Another point of interest is a very close agreement between the NSCAPW bands and the SCOPW (self-consistent orthogonalized-plane-wave) bands of Stukel *et al.*[45-47] The latter were obtained using $\alpha = 1.0$ although Stukel *et al.* have also performed calculations with $\alpha = 0.66$ (Kohn-Sham[48] exchange value). Their experience was that non-self-consistent Kohn-Sham exchange calculations did indeed agree with experiments better than did the self-consistent ones. The opposite was true of the bands using the Slater $\alpha = 1.0$ exchange.[49] They attribute this to the fact that the Slater exchange may have the effect of including some correlation as well.

A quantitative comparison of the present bands, a selected set of other calculations, and experiment is given in Table III. The SCAPW valence band is about 1 eV too narrow but the rest of the valence bands at symmetry points are within experimental error bars. In contrast, the SCAPW band gap is 1 eV too high and the Γ_2', Γ_{15} level ordering is interchanged. The usual trend is to underestimate the band gap.[1,2] The reason must be intricately involved in the treatment of the exchange-correlation potential.

The trend for underestimating the band gap using α close to the Kohn-Sham value of 0.66 is by no means universal. Stukel *et al.*[45-47] found this to be true for Si but in analogous calculations for Ge (Ref. 46) and GaAs (Ref. 47) the Kohn-Sham exchange gave larger fundamental gaps than the Slater exchange. The band-gap variation is evidently a complicated function of band-edge locations, wave-function symmetry, self-consistent treatment, and, of course, the exchange-correlation potential.

As a limited test of the above hypotheses I used the final charge density and constructed another potential using $\alpha = 0.66$. This calculation is by no means self-consistent but should exhibit relevant trends. It was found that the $X_{1,c} - \Gamma'_{25,v}$ gap went from 2.28 to 1.73 eV, consistent with Stukel *et al.* findings.[46,47] Similarly, $\Gamma_{15,c} - \Gamma'_{25,v}$ decreased from 3.30 to 3.02 eV while the $\Gamma'_{2,c} - \Gamma'_{25,v}$ increased from 2,38 to 2.70 eV. All these trends agree with those found by Stukel *et al.* in going

TABLE III. Comparison of the present non-self-consistent (NSCAPW) and self-consistent (SCAPW) silicon eigenvalues (in eV) with calculations of Zunger and Cohen (Ref. 2), Stukel and Euwema (Ref. 45, $\alpha = 1$), Hamann (Ref. 1), Chelikowsky and Cohen (Ref. 6), and experiment.

	NSCAPW	SCAPW	Zunger and Cohen	Stukel and Euwema	Hamann	Chelikowsky and Cohen	Experimental
Γ_1	−11.76	−11.44	−12.20	−11.74	−12.02	−12.36	−12.4 ± 0.6 [a]
Γ'_{25}	0.00	0.00	0.00	0.00	0.00	0.00	
Γ_{15}	2.82	3.30	2.48	2.79	2.49	3.42	
Γ'_2	2.83	2.38	2.50	2.75	3.18	4.10	4.15 ± 0.05, [b] 4.21 ± 0.02 [c]
Γ_1		10.37	7.25		7.46	7.69	~7.6 [b]
Γ'_{12}	8.28	9.09			7.86	8.19	
X_1	−7.77	−7.66	−8.02	−7.75	−7.84	−7.69	
X_4	−2.63	−2.34	−2.93	−2.72	−2.82	−2.86	−2.9, [b] −2.5 ± 0.3 [d]
X_1	1.27	2.28	0.52	1.28	0.55	1.17	1.13 [e]
X_4		9.73	9.97	9.79	10.32		
L'_2	−9.57	−9.42	−9.92	−9.53	−9.64	−9.55	−9.3 ± 0.4 [d]
L_1	−6.71	−6.33	−7.21	−6.75	−7.06	−6.96	−6.4 ± 0.4, [a] −6.8 ± 0.2 [d]
L'_3	−1.12	−1.03	−1.28	−1.18	−1.16	−1.23	−1.2 ± 0.2 [b]
L_1	1.59	1.95	1.13	1.60	1.40	2.23	2.04 ± 0.06 [f]
L_3	3.79	4.47	3.36	3.83	3.37	4.34	3.9 ± 0.1 [b]
Band gap	1.12	2.06	0.5	1.10			1.12 [g]

[a] Reference 50.
[b] Reference 51.
[c] Reference 52.
[d] Reference 53.
[e] Reference 54.
[f] Reference 55.
[g] Reference 56.

from $\alpha = 1.0$ to $\alpha = 0.66$. This is also testimony to the fact that one-parameter variation cannot improve all energy separations to yield agreement with experiment.

In order to test various non-MT approximations, the Si bands were calculated first in the WMT scheme and then with a flat interstitial potential. Table IV displays the results. The flat-potential approximation is the more drastic of the two, deviating by about 1.5 eV from the non-MT results. The WMT eigenvalues are shifted by typically 0.2 eV. This further attests to the inadequacy of non-MT calculations for directionally bonded semiconductors.

TABLE IV. Comparison of the non-muffin-tin SCAPW eigenvalues (in eV) with the calculations using the self-consistent potential without nonspherical MT corrections (WMT), and with the flat interstitial potential.

Level	Non-MT SCAPW	WMT	Flat PW potential
Γ_1	−11.43	−11.34	−10.48
Γ'_{25}	0.00	0.32	1.41
Γ'_2	2.38	2.22	2.67
Γ_{15}	3.30	3.12	4.29
Γ'_{12}	9.09	9.00	>10.4

IV. CONCLUSIONS

The Rudge APW formalism has been applied to silicon without any shape approximations for the potential. The scheme was shown to be computationally tractable and relatively easy to apply. After the initial effort in calculating the Ewald sums the method turned out to be as easy to apply as the traditional APW technique. The iteration toward self-consistency has been carried out as well since Rudge's formalism has this important feature built in.

The self-consistent band-structure results agree very well for the valence band with available experimental data. The discrepancy between the conduction band and the data can be directly attributed to our lack of knowledge of potentials to be used for excited-state properties of materials. On the other hand the non-self-consistent APW bands are in better agreement with experiments and empirical pseudopotential results for the conduction bands.

ACKNOWLEDGMENTS

This work was performed under Contract No. F33615-78-C-5064 at the Materials Laboratory, Air Force Wright Aeronautical Laboratories, Wright-Patterson Air Force Base, Dayton, Ohio. The author is grateful for support throughout all stages of this work to Mr. John Detrio of the University of Dayton and the AFWAL/MLPO-WPAFB personnel.

[1]D. R. Hamann, Phys. Rev. Lett. 42, 662 (1979).
[2]A. Zunger and M. L. Cohen, Phys. Rev. B 20, 4082 (1979).
[3]E. O. Kane, Phys. Rev. B 4, 1910 (1971).
[4]J. C. Inkson and M. Bennett, J. Phys. C 10, 987 (1977); 11, 2017 (1978).
[5]W. Hanke and L. J. Sham, Phys. Rev. Lett. 43, 387 (1979).
[6]J. R. Chelikowsky and M. L. Cohen, Phys. Rev. B 10, 5095 (1974).
[7]P. D. DeCicco, Phys. Rev. 153, 931 (1967).
[8]D. D. Koelling, Phys. Rev. 188, 1049 (1969).
[9]H. Schlosser and P. M. Marcus, Phys. Rev. 131, 2529 (1963).
[10]L. F. Mattheiss, Phys. Rev. 181, 987 (1969).
[11]D. D. Koelling and A. J. Freeman, Phys. Rev. B 7, 4454 (1973).
[12]D. D. Koelling, A. J. Freeman, and F. M. Mueller, Phys. Rev. B 1, 1318 (1970).
[13]B. M. Klein, L. L. Boyer, and D. A. Papaconstantopoulos, Phys. Rev. B 18, 6411 (1978).
[14]W. E. Rudge, Phys. Rev. 181, 1020 (1969); 181, 1024 (1969).
[15]E. O. Kane, Phys. Rev. B 4, 1917 (1971).
[16]L. Kleinman and R. Shurtleff, Phys. Rev. 188, 1111 (1969); Phys. Rev. B 4, 3284 (1971).
[17]R. Shurtleff and L. Kleinman, Phys. Rev. B 3, 2418 (1971).
[18]L. Dagens and F. Perrot, Phys. Rev. B 8, 1281 (1973).
[19]N. Elyashar and D. D. Koelling, Phys. Rev. B 13, 5362 (1976); 15, 3620 (1977).
[20]A. T. van Kessel, H. W. Myron, and F. M. Mueuller, Phys. Rev. Lett. 41, 181 (1978).
[21]R. Keown, Phys. Rev. 150, 568 (1966).
[22]D. A. Papaconstantopoulos and B. M. Klein, Solid State Commun. 34, 511 (1980).
[23]O. K. Anderson, Phys. Rev. B 12, 3060 (1975).
[24]J. Korringa, Physica (Utrecht) 13, 392 (1947).
[25]W. Kohn and N. Rostoker, Phys. Rev. 94, 1111 (1954).
[26]J. H. Wood, Phys. Rev. 126, 517 (1962).
[27]L. F. Mattheiss, J. H. Wood, and A. C. Switendick, in *Methods of Computational Physics*, edited by B. Alder *et al.* (Academic, New York, 1969), Vol. VIII, p. 64.
[28]G. F. Koster, Solid State Phys. 5, 173 (1957).
[29]J. C. Slater, Rev. Mod. Phys. 37, 68 (1965).
[30]A. C. Hurley, Philos. Trans. R. Soc. London 260A, 1108 (1966).
[31]V. Heine, *Group Theory in Quantum Mechanics* (Pergamon, New York, 1960).
[32]J. D. Slater, *Quantum Theory of Molecules and Solids* (McGraw-Hill, New York, 1965), Vol. II, p. 368.
[33]J. C. Slater, Phys. Rev. 51, 846 (1937).
[34]T. L. Loucks, *Augmented Plane Wave Method* (Benjamin, New York, 1967).
[35]L. F. Mattheiss, Phys. Rev. 133, A1399 (1964).
[36]J. P. Desclaux, Comput. Phys. Commun. 1, 216 (1969).
[37]F. C. Von der Lage and H. A. Bethe, Phys. Rev. 71, 612 (1947).
[38]P. O. Löwdin, Adv. Phys. 5, 1 (1956).
[39]F. Szmulowicz, preceding paper, Phys. Rev. B 23, 1646 (1981).
[40]M. L. Cohen, M. Schlüter, J. R. Chelikowsky, and S. G. Louie, Phys. Rev. B 12, 4000 (1975); 12, 5575 (1975); S. G. Louie and M. L. Cohen, *ibid.* 13, 2461 (1976); S. G. Louie, M. Schlüter, J. R. Chelikowsky, and M. L. Cohen, *ibid.* 13, 1654 (1976); M. Schlüter, A. Zunger, G. Kerker, K. M. Ho, and M. L. Cohen, Phys. Rev. Lett. 42, 540 (1979).
[41]E. Wigner, Phys. Rev. 46, 1002 (1934).
[42]R. N. Euwema, D. J. Stukel, and T. C. Collins, in *Computational Methods in Band Theory*, edited by P. M. Marcus *et al.* (Plenum, New York, 1971), p. 82.
[43]J. H. Wilkinson, *The Algebraic Eigenvalue Problem* (Oxford University Press, New York, 1965).
[44]J. P. Walter and M. L. Cohen, Phys. Rev. B 4, 1877 (1971).
[45]D. J. Stukel and R. N. Euwema, Phys. Rev. B 1, 1635 (1970).
[46]D. J. Stukel, Phys. Rev. B 3, 3347 (1971).
[47]D. J. Stukel, R. N. Euwema, T. C. Collins, and V. H. Smith, Jr., Phys. Rev. B 1, 779 (1970).
[48]W. Kohn and L. J. Sham, Phys. Rev. 140, A1333 (1965); R. Gaspar, Acta Phys. Acad. Sci. Hung. 3, 263 (1954).
[49]J. C. Slater, Phys. Rev. 81, 386 (1951).
[50]W. D. Grobman and D. E. Eastman, Phys. Rev. Lett. 29, 1508 (1972).
[51]W. E. Spicer and R. C. Eden, in *Proceedings of the Ninth International Conference on the Physics of Semiconductors, Moscow, 1968,* edited by S. M. Ryvkin *et al.* (Nauka, Leningrad, 1968), Vol. 1, p. 65.
[52]D. E. Aspnes and A. A. Studna, Solid State Commun. 11, 1375 (1972).
[53]L. Ley, S. Kowalczyk, R. Pollak, and D. A. Shirley, Phys. Rev. Lett. 29, 1088 (1972).
[54]M. Walkowsky and R. Braunstein, Phys. Rev. B 5, 497 (1972); R. R. Zucca, J. P. Walter, Y. R. Shen, and M. L. Cohen, Solid State Commun. 8, 627 (1970).
[55]R. Hulthen and N. G. Nillson, Solid State Commun. 18, 1341 (1976).
[56]A. Frova and P. Handler, Phys. Rev. Lett. 14, 178 (1965).